Proceedings of the
Annual Stability Conference
Structural Stability Research Council
Pittsburgh, Pennsylvania, May 10-14, 2011

The Natural Period as an Indicator of Second-Order Effects

D.E. Statler[1], R.D. Ziemian[2], L.E Robertson[3]

Abstract

The results of a recent study that investigates using a structure's natural period to predict moment amplification due to second-order effects in beam-columns of steel moment-resisting frames is presented. Using a simplified structural model, two second-order moment amplification expressions are developed that are based on the natural period of the system. The accuracy of these expressions is then evaluated through the use of 9 two-dimensional frames selected from benchmark studies previously presented in the literature—with the addition of three modifications of the aforementioned frames that serve to broaden the scope of buildings investigated. These frames, ranging from one to forty stories, include a wide range of height-to-width aspect ratios. In all cases, predicted results are compared with more "exact" solutions obtained from second-order finite element analyses, as well as traditional moment amplification factors calculated by the approximate story-stiffness approach. It is shown that the natural period can be used to accurately predict the significance of second-order effects and hence, could be quite useful to the structural engineer during preliminary and intermediate stages of design.

1. Introduction

Second-order forces and moments develop in structural members as a consequence of formulating equilibrium on the deformed geometry. For example, when wind forces displace a slender building laterally, an additional overturning moment is produced by the displaced weight of the building. Because the development of these additional stresses correspond to the development of additional strains, the process is self-stoking, and can lead to force and moment demands significantly larger than those predicted from an equilibrium analysis of the undeformed structure.

The simple example above describes the P-Δ effect. It should be noted that another form of second-order effects, P-δ, refers to the influence of axial force on the flexural stiffness of an

[1] Graduate Student, Dept. of Civil and Environmental Engineering, Lehigh University
[2] Professor, Dept. of Civil and Environmental Engineering, Bucknell University, <ziemian@bucknell.edu>
[3] Director of Design, Leslie E. Robertson Associates

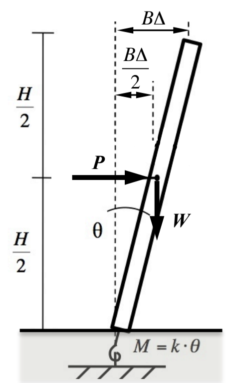

Figure 1: Deformed shape of simplified structural model.

individual structural member. The approximate moment amplification expressions presented in this paper are concerned solely with P-Δ effects.

Robertson (1981) presented a theoretical relationship between the natural period of a structure and an amplification factor describing the P-Δ induced overturning moment. Because the natural period of a structure is well understood and can be easily and accurately approximated, this paper examines the potential for using such a method to predict second-order effects in individual members. Using a population of twelve moment-resisting frames selected (and in some cases modified) from benchmark studies previously presented in the literature, predictions based upon two variations of Robertson's concept are compared for accuracy with rigorous second-order finite element analysis and traditional moment amplification factors calculated by the well-established story stiffness approach.

2. Theory

2.1 Amplification Factor

Figure 1 shows a structure, with center of mass located at the centroid, in a highly simplified linear deformed shape. The lateral force P has displaced the building of height H by a distance Δ and corresponding angle θ from the original vertical position. The overturning moment generated by the displaced weight of the building W increases this lateral displacement by an amplification factor B.

The total moment (including both first- and second-order effects) at the base of the structure is

$$M = P\frac{H}{2} + W\frac{B\Delta}{2} \tag{1}$$

Defining the angular stiffness k as the moment developed at the base of the structure due to a unit rotation, and assuming small angles, this total moment can be rewritten in terms of the first-order moment M_1 (= $PH/2$) and the height H, weight W, and base stiffness k as follows

$$k = \frac{M}{\theta} \tag{2}$$

$$tan(\theta) = \frac{B\Delta}{H} \approx \theta \tag{3}$$

Substituting Eq. 3 into Eq. 2, and the resulting expression for $B\Delta$ into Eq. 1 gives

$$M = P\frac{H}{2} + W\frac{HM}{2k} \tag{4}$$

which may be expressed as

$$M\left(1 - \frac{WH}{2k}\right) = P\frac{H}{2} = M_1 \tag{5}$$

The moment amplification factor B can then be defined as

$$B = \frac{M}{M_1} = \frac{1}{1 - \frac{WH}{2k}} \tag{6}$$

2.2 Natural Period

The oscillation of the structure shown in Fig. 1 can be modeled by a single degree of freedom spring-mass system (Fig. 2). Assuming no damping, dynamic equilibrium of the moment about the base gives

$$\frac{mH^2}{3}\ddot{\theta} + k\theta = 0 \tag{7}$$

The fundamental period of this system is

$$T = 2\pi\sqrt{\frac{mH^2}{3k}} \tag{8}$$

or, with $m = W/g$

$$T_A = 2\pi\sqrt{\frac{WH^2}{3gk}} \tag{9}$$

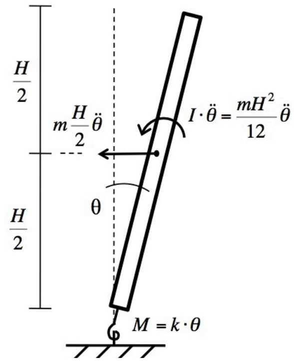

Figure 2: Single degree of freedom spring-mass system.

This expression neglects the *P*-Δ effect, which effectively reduces the stiffness of the system by the inverse of the moment amplification factor *B*. Dividing the stiffness *k* by the moment amplification factor results in a *P*-Δ corrected natural period

$$T_B = 2\pi\sqrt{\frac{BWH^2}{3gk}} \tag{10}$$

2.3 Proposed Models

The expressions developed for the moment amplification factor (Eq. 6) and the natural period (Eqs. 9 and 10) share many of the same structural parameters. By first solving Eqs. 9 and 10 for the weight of the structure *W*, and then substituting into Eq. 6, the following moment amplification factors may be obtained that are in terms of the natural period of the system

$$B_A = \frac{1}{1-\frac{3gT^2}{8\pi^2 H}} \tag{11}$$

$$B_B = 1+\frac{3gT^2}{8\pi^2 H} \tag{12}$$

with the latter expression (Eq. 12) including the *P*-Δ correction.

3. Methodology

3.1 Model Frames

With the intent of representing a wide variety of structural geometries and loadings, the steel moment frames investigated in this study were selected from frames previously presented in the literature. When possible, the structural geometry, member sizes, material properties, support, and loading conditions have been duplicated from the source studies. Deviations from these studies were only made to be consistent with current LRFD procedures and when the original member sizes were no longer available.

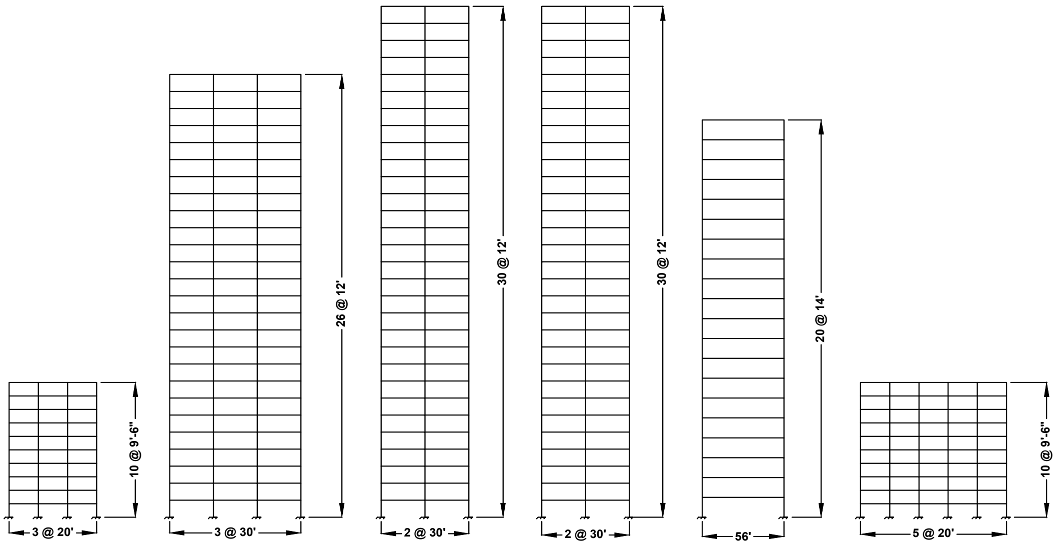

	Frame 1	Frame 2	Frame 3	Frame 4	Frame 5	Frame 6
Stories / Bays	10 / 3	26 / 3	30 / 2	30 / 2	20 / 1	10 / 5
Frame Spacing (ft)	20	30	30	30	30	20
Roof Load (psf)						
Live	30	30	40	30	30	30
Dead	40	40	50	40	40	40
Floor Load (psf)						
Live	40	75	100	75	75	40
Dead	50	50	75	50	50	55
Wall Load (kip/story)	9.5	18	24	18	18	9.5
Wind Load (psf)	16.25	16.25	16.25	16.25	16.25	16.25
Natural Period (s)	2.74	5.44	6.1	5.76	4.58	3.05

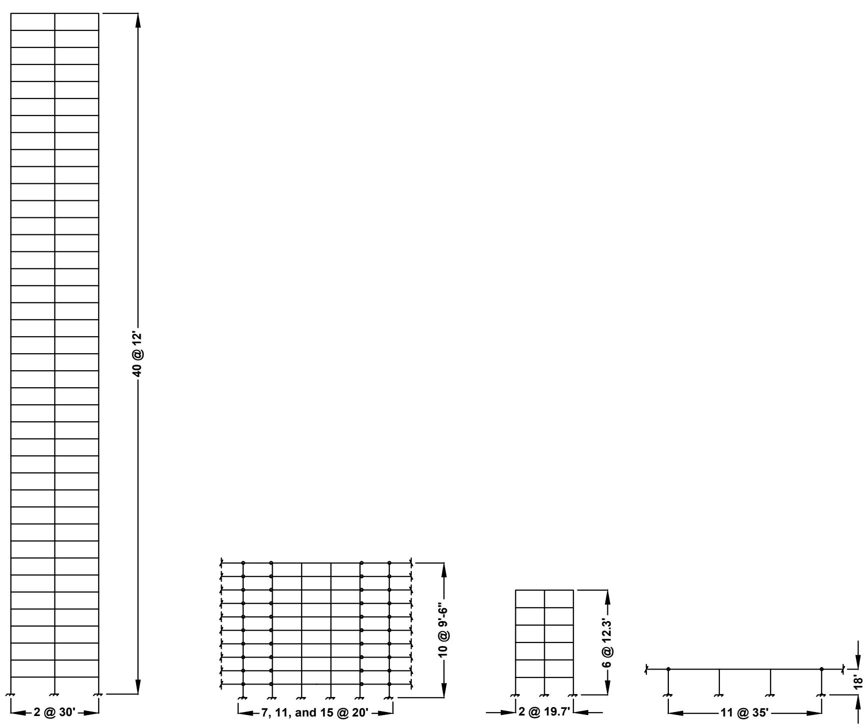

	Frame 7	Frames 8 - 10	Vogel Frame	Factory Frame
Stories / Bays	40 / 2	10 / 7, 11, 15	6 / 2	1 / 11
Frame Spacing (ft)	30	20	19.7	35
Roof Load (psf)				
Live	30	30	110	40
Dead	40	40	(Factored)	80
Floor Load (psf)				
Live	75	40	171	N/A
Dead	50	50	(Factored)	N/A
Wall Load (kip/story)	18	9.5	N/A	N/A
Wind Load (psf)	16.25	16.25	19	16.25
Natural Period (s)	6.95	3.96, 4.88, 5.66	2.58	3.01

Figure 3: Frame descriptions

Figure 3 contains descriptions of the frame geometries and loading conditions studied. Frames 1-7 are taken from a study by Lu, et al. (1975) and represent a wide variety of low- to high-rise office and apartment-style steel structures. Frames 8, 9, and 10 are variations of Frame 1 that include an increasing number of leaning columns (4, 8, and 12 leaning bays) and hence, provide the opportunity to study intermediate ratios of natural period to building height. More specific details of the frames, including member sizes, are provided by Statler (2010).

The "Vogel Frame" is a 6-story, 2-bay frame taken from a calibration study by Vogel (1985). The "Factory Frame", which was studied by Deierlein (2003), consists of a single-story 11-bay structure that includes ten leaning columns. This frame is included as an example of a low-rise industrial building in which low wind exposure and heavy equipment suspended from the ceiling contribute to large second-order effects (Springfield, 1991).

3.2 Additional Details of the Finite Element Models

When service loads were specified in the referenced frame studies, the LRFD load combination $1.2D + 0.5L + 1.6W$ was applied. All distributed loads were lumped to beam-column intersections using tributary area (lengths), and self-weight was assumed to be included in the dead loads provided.

Material inelasticity, residual stresses, and connection size and stiffness have been neglected for simplicity. All wide-flange sections are oriented for major-axis flexure (i.e., with their webs in the plane of the frame) and all out-of-plane behavior is restrained. Member lengths are defined by their centerlines. To adequately account for P-δ effects, members are divided into four elements. Second-order analyses were performed using a predictor-corrector (mid-point Runge-Kutta) solution scheme and applying the factored loads in 5% increments until the frame is fully loaded.

3.3 Procedure

For each frame investigated, internal member forces and moments were obtained from first- and second-order elastic finite element analyses (Ziemian and McGuire, 2009) using factored gravity and wind load combinations. Of particular interest to this study are the internal moments observed at the ends of all beam-column members that comprise the lateral force-resisting system. Using the results of these analyses, the "exact" amplification factors for each member are then calculated as the ratio of their second- to first-order moments.

As might be expected, using the finite element analyses to calculate ratios of second- to first-order internal moments can result in some spurious results. For example, an extraordinarily large ratio can be computed for a case where the magnitude of a member's second-order moment is small, but the magnitude of its first-order moment is much smaller or near zero. Likewise, accounting for nonlinear behavior can produce differences in sign between the first- and second-order moments at the ends of a given member. In these cases, the moment amplification is typically not of consequence in the design of the structure because the second-order (and first-order) moment is well below the design resistance of the member. In this regard, the ratios of the members' second-order moments to their plastic moment capacities can be used as a metric for determining the significance of the moment amplification factors that are back-calculated from

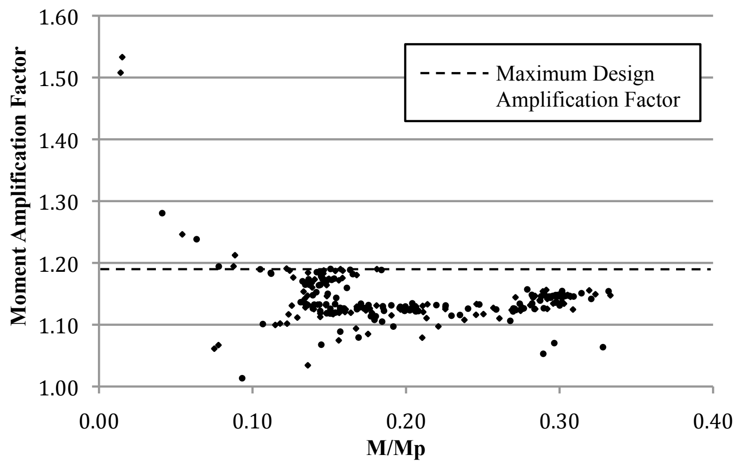

Figure 4: Distribution of moment amplification factors – Frame 7

first- and second-order finite element analyses. As an example, Figure 4 shows a plot of the maximum "exact" moment amplification factors for all beam-columns in Frame 7 versus their respective normalized second-order moments (M/M_p). For the above-mentioned reasons, some members have relatively small moments but very large amplification factors. As shown, these spurious or misleading amplification factors tend to stop appearing for M/M_p ratios larger than about 0.05 to 0.10.

For each of the frames investigated, plots similar to the one shown in Fig. 4 were prepared and are provided in Appendix 1. For each population of moment amplification factors (which includes data points for each end of all beam-columns in the frame), the average and standard deviation was computed for comparison with the proposed methods.

The same finite element program was also used to compute the fundamental periods of the structures and load cases by solving the eigenvalue problem

$$\left| K - \omega^2 M \right| = 0 \tag{13}$$

in which the smallest modal frequency corresponds to the fundamental period. The first-order elastic stiffness matrix K is employed and the mass matrix M is formed by converting all factored gravity loads to equivalent masses. It should be noted that because the mass matrix is calculated from factored loads, this approach predicts a longer natural period than is likely to be observed in the structure during service.

With the height and natural period for each frame, the amplification factors given by Eqs. 11 and 12 are then calculated. These natural period-based amplification factors, B_A and B_B, are then compared with the "exact" amplification factors obtained by rigorous finite element analysis. Such results are also compared with B_2 amplification factors calculated according to the story stiffness approach provided in Section C2.1b of the AISC *Specification for Structural Steel Buildings* (2005). For example, superimposed on the plot in Fig. 4 is the largest of the AISC story-based amplification factors (1.19) for all stories within Frame 7. In general, the average of the B_2 amplification factors for all stories within a frame was used to serve as an additional measure for assessing the accuracy of the proposed models with respect to current design practice.

4. Results

Table 1 presents a summary of the results obtained in this study. For each frame, the average and standard deviation of the "exact" analytical moment amplification B and the story-stiffness B_2 amplification factors are presented for comparison with the amplification factors estimated by the proposed models B_A and B_B, which again are only a function of the frames' heights and fundamental periods. This data is provided for the ends of all beam-columns ("All-Inclusive") and for only those ends with M/M_p exceeding 10%.

Several observations can be made from the results present in Table 1, including

1. Comparing the proposed amplification factors (Eqs. 11 and 12), the P-Δ uncorrected natural period B_A provides consistently higher moment amplification estimates than the P-Δ corrected model B_B.
2. Both of the proposed factors (B_A and B_B) agree fairly well with the average of the amplification factors B obtained from rigorous second-order finite element analyses. The variation, however, does increase for frames with greater ratios of natural period to frame height.
3. Good agreement is also observed when making similar comparisons with the story-stiffness B_2 amplification factors, although in general the story-stiffness method does tend to provide more conservative predictions.

Figure 5 conveys the data from Table 1 in graphical form, with Eqs. 11 and 12 shown as continuous curves and the average analytical moment amplification factors ($M/M_p > 0.10$) plotted as data points for each frame. The error bars represent the range of observed moment amplification for all beam-columns with M/M_p exceeding 10%.

Table 1: Summary of results

Frame Parameters			**F.E. Analytical Data Avg. *B* (Std.Dev.)**		**Models**				**AISC Design B_2**	
					B_A		**B_B**			
Name	**T_n (s)**	**H (ft)**	**All-Inclusive**	**M/M_P > 10%**	**Avg.**	**% Err.**	**Avg.**	**% Err.**	**Avg. (Std.Dev.)**	**% Err.**
Frame 1	2.74	95	1.09 (0.03)	1.10 (0.02)	1.11	0.9%	1.10	0.0%	1.11 (0.04)	0.9%
Frame 2	5.44	312	1.12 (0.04)	1.12 (0.02)	1.13	0.9%	1.12	0.0%	1.14 (0.03)	1.8%
Frame 3	6.1	360	1.13 (0.18)	1.13 (0.04)	1.14	0.9%	1.13	0.0%	1.16 (0.04)	2.7%
Frame 4	5.76	360	1.11 (0.04)	1.12 (0.02)	1.13	0.9%	1.11	-0.9%	1.14 (0.03)	1.8%
Frame 5	4.58	280	1.09 (0.03)	1.10 (0.02)	1.10	0.0%	1.09	-0.9%	1.11 (0.04)	0.9%
Frame 6	3.05	95	1.12 (0.05)	1.13 (0.03)	1.14	0.9%	1.12	-0.9%	1.14 (0.06)	0.9%
Frame 7	6.95	480	1.14 (0.05)	1.14 (0.03)	1.14	0.0%	1.12	-1.8%	1.16 (0.03)	1.8%
Frame 8	3.96	95	1.21 (0.12)	1.24 (0.06)	1.25	0.8%	1.20	-3.2%	1.27 (0.09)	2.4%
Frame 9	4.88	95	1.37 (0.19)	1.40 (0.11)	1.44	2.9%	1.31	-6.4%	1.49 (0.19)	6.4%
Frame 10	5.66	95	1.59 (0.25)	1.63 (0.20)	1.70	4.3%	1.41	-13.5%	1.81 (0.36)	11.0%
Vogel	2.58	73.82	1.11 (0.03)	1.12 (0.02)	1.12	0.0%	1.11	-0.9%	1.13 (0.03)	0.9%
Factory	3.01	18	1.71 (0.07)	1.71 (0.07)	2.59	51.5%	1.61	-5.8%	1.95 (N/A)	14.0%

% Err. = $100 \times (B_i - B)/B$

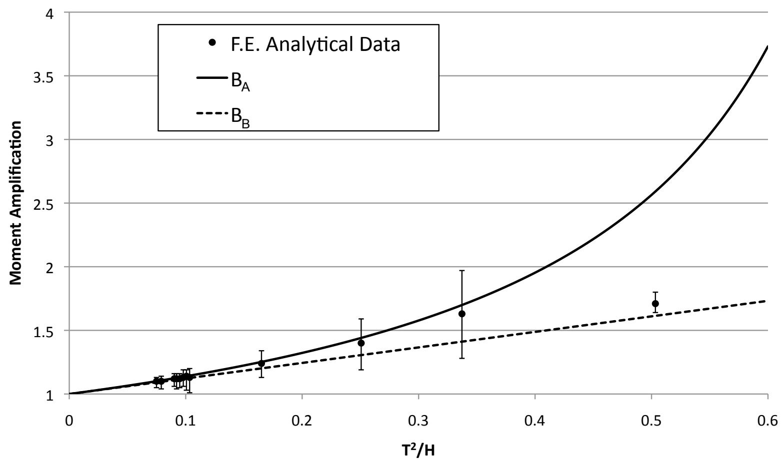

(a)

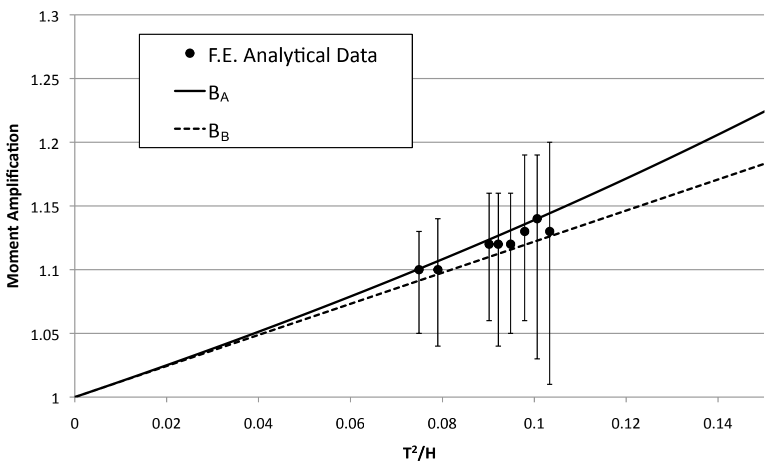

(b)

Figure 5: Plot of results

The figures make apparent the expanding difference between the proposed approximations at higher ratios of natural period to frame height. It is of interest to note that at the highest ratio investigated—that of the Factory Frame—the observed results are much closer to B_B (Eq. 12) than to B_A (Eq. 11). On the other hand, the trend in Frames 8-10 (comprising the central three data points above) tracks more in the direction of B_A. With the exception of the Factory Frame, the magnitude of the observed range in moment amplification is correlated positively with the ratio of natural period to frame height. This disparity for the Factory Frame may relate to the redundancy of the lateral system, which consisted of only two beam-columns (i.e., limited available data).

From Fig. 5b, which provides an enlarged view of the results for Frames 1-7 and the Vogel Frame, it can be seen that for more typical ratios of natural period squared to frame height, Eqs. 11 and 12 agree fairly closely with the finite element results.

The general trend in the data indicates that the P-Δ uncorrected natural period model B_A and the P-Δ corrected model B_B provide good upper- and lower-bound estimates of moment amplification, respectively. In other words, conservative estimates of the influence of second-order effects can be obtained consistently with B_A, while potentially more accurate estimates can obtained with B_B.

5. Conclusions

It has been shown that the height and natural period of a steel moment frame structure can be used in relatively simple equations to accurately predict the average influence of second-order effects. Although these equations were originally established to estimate moment amplification at the base of a structure, this study shows that they can also be used to predict the average moment amplification occurring in all beam-columns within a given frame.

Although more simple to compute, these approximations provide only a single average value for the entire system and not amplification factors for individual stories or components. This approximation, however, could be quite useful during preliminary and intermediate stages of design, especially when needing to make informed decisions regarding the potential impact of second-order effects.

References

AISC. Steel Construction Manual, 13th Edition. 2006.

Deierlein, G., (2003), "Background and Illustrative Examples on Proposed Direct Analysis Method for Stability Design of Moment Frames." Report of AISC TC 10. July 13, 2003.

Lu, L.W., Ozer, E., Daniels, J.H., Okten, O.S., and Morino, S. (1975), "Frame Stability and Design of Columns in Unbraced Multistory Steel Frames", Fritz Engineering Laboratory Report No. 375.2, Lehigh University, Bethlehem, Pennsylvania, July, 1975.

Robertson, L.E., (1981), "The P-delta Phenomenon as evaluated by the Fundamental Period of Oscillation," Construction Metallique, 3-1981.

Springfield, J. (1991), "Limits on Second-Order Elastic Analysis," Proc. SSRC Annu. Tech. Sess., SSRC, Bethlehem, PA, 89-99.

Statler, D.E. (2010), "Using the Natural Period of a Structure as an Indicator of the Significance of Second-Order Effects," Honors Thesis, Bucknell University, Lewisburg, PA.

Vogel, U. (1985), "Calibrating Frames", Stahlbau, Vol. 10, pp 295-301.

Ziemian, R.D. and McGuire, W. (2009) *MASTAN2*., www.mastan2.com.

Appendix 1. Comparative Results for All Frames.

Legend:

- B_A (solid line)
- B_B (dashed line)
- F.E. Analytical Data (dots)

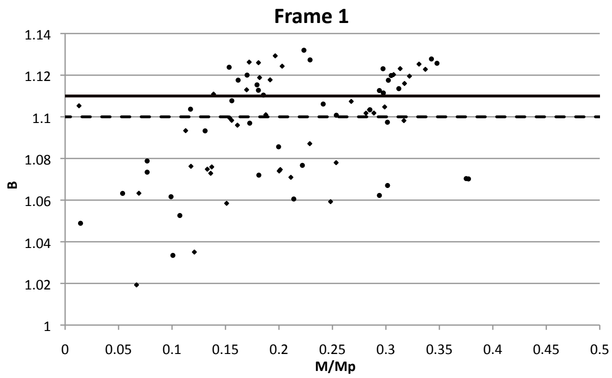

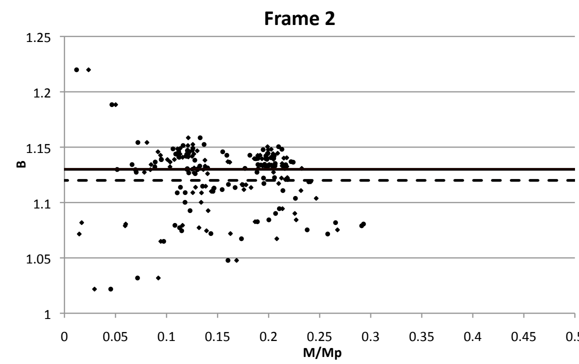

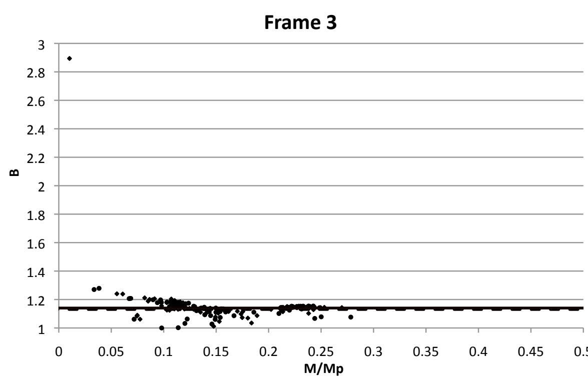

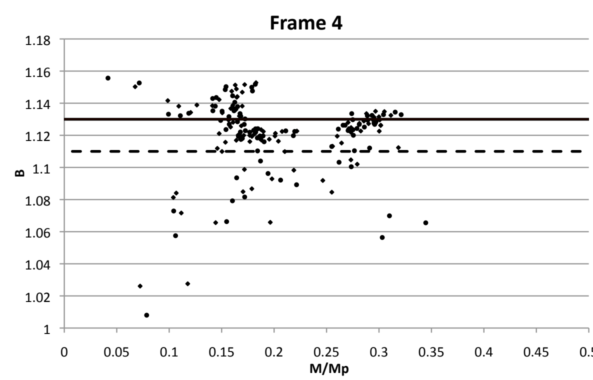

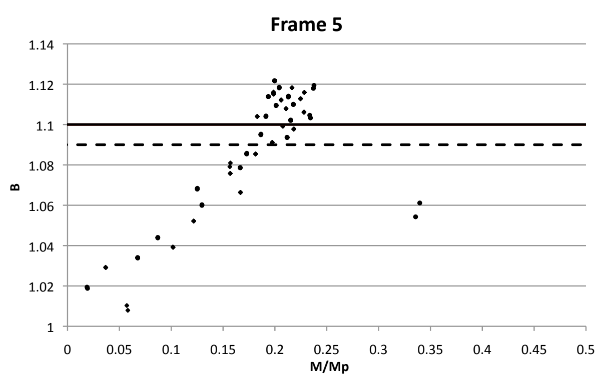

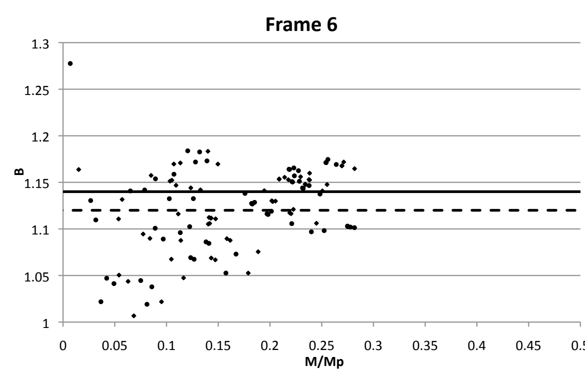

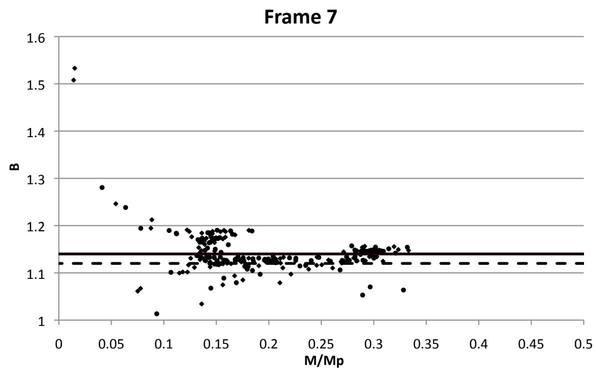
Frame 7
B
M/Mp

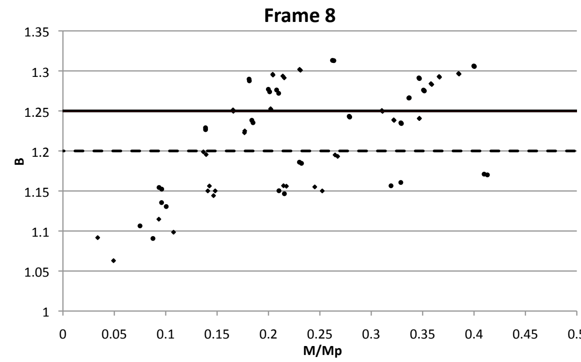
Frame 8
B
M/Mp

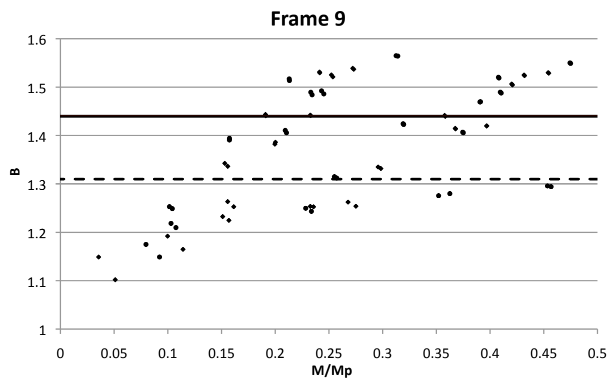
Frame 9
B
M/Mp

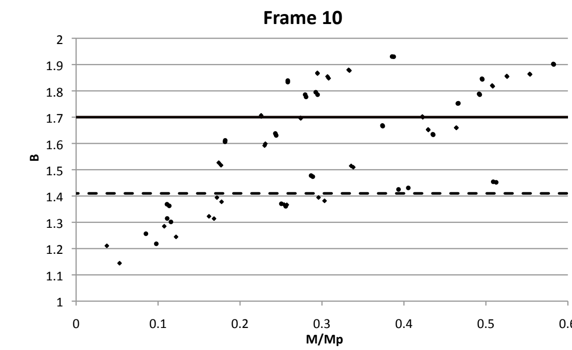
Frame 10
B
M/Mp

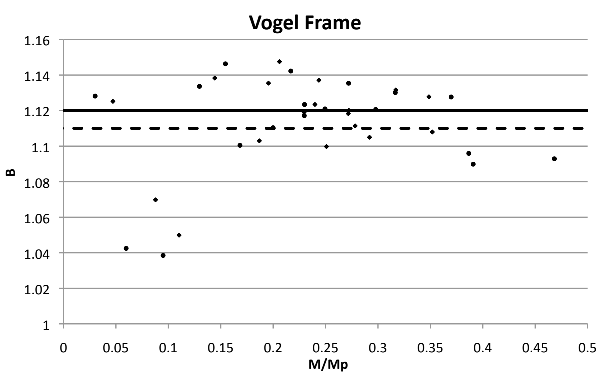
Vogel Frame
B
M/Mp

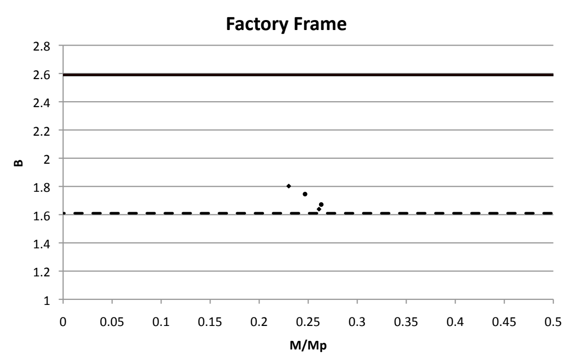
Factory Frame
B
M/Mp